

Light-Front Holography and AdS/QCD: A First Approximation to QCD

Stanley J. Brodsky

SLAC National Accelerator Laboratory

Stanford University, Stanford, CA 94309, USA

and

Guy F. de Téramond

Universidad de Costa Rica

San José, Costa Rica

Abstract

The combination of Anti-de Sitter space (AdS) methods with light-front holography leads to a semi-classical first approximation to the spectrum and wavefunctions of meson and baryon light-quark bound states. Starting from the bound-state Hamiltonian equation of motion in QCD, we derive relativistic light-front wave equations in terms of an invariant impact variable ζ which measures the separation of the quark and gluonic constituents within the hadron at equal light-front time. These equations of motion in physical space-time are equivalent to the equations of motion which describe the propagation of spin- J modes in anti-de Sitter (AdS) space. Its eigenvalues give the hadronic spectrum, and its eigenmodes represent the probability distribution of the hadronic constituents at a given scale. Applications to the light meson and baryon spectra are presented. The predicted meson spectrum has a string-theory Regge form $\mathcal{M}^2 = 4\kappa^2(n + L + S/2)$; *i.e.*, the square of the eigenmass is linear in both L and n , where n counts the number of nodes of the wavefunction in the radial variable ζ . The space-like pion form factor is also well reproduced. One thus obtains a remarkable connection between the description of hadronic modes in AdS space and the Hamiltonian formulation of QCD in physical space-time quantized on the light-front at fixed light-front time τ . The model can be systematically improved by using its complete orthonormal solutions to diagonalize the full QCD light-front Hamiltonian or by applying the Lippmann-Schwinger method in order to systematically include the QCD interaction terms.

Work supported in part by US Department of Energy contract DE-AC02-76SF00515.

1 Introduction

The Schrödinger equation plays a central role in atomic physics, providing a simple, but effective, first approximation description of the spectrum and wavefunctions of bound states in quantum electrodynamics. It can be systematically improved in QED, leading to an exact quantum field theoretic description of atomic states such as positronium and muonium as given by the relativistic Bethe-Salpeter equation.

We have recently shown that the combination of Anti-de Sitter space (AdS) methods with light-front holography lead to a remarkably accurate first approximation for the spectrum and wavefunctions of meson and baryon light-quark bound states. The resulting equation for a meson $q\bar{q}$ bound state at fixed light-front time $\tau = t + z/c$, the time marked by the front of a light wave, [1] has the form of a relativistic Lorentz invariant Schrödinger equation

$$\left(-\frac{d^2}{d\zeta^2} - \frac{1 - 4L^2}{4\zeta^2} + U(\zeta) \right) \phi(\zeta) = \mathcal{M}^2 \phi(\zeta), \quad (1)$$

where the confining potential is $U(\zeta) = \kappa^4 \zeta^2 + 2\kappa^2(L + S - 1)$ in a soft dilaton modified background. There is only one parameter, the mass scale $\kappa \sim 1/2$ GeV, which enters the confinement potential. Here $S = 0, 1$ is the spin of the q and \bar{q} , L is their relative orbital angular momentum and $\zeta = \sqrt{x(1-x)b_\perp^2}$ is a Lorentz invariant coordinate that measures the distance between the quark and antiquark; it is analogous to the radial coordinate r in the Schrödinger equation. One thus obtains a remarkable connection between the description of hadronic modes in AdS space and the Hamiltonian formulation of QCD in physical space-time quantized on the light-front (LF) at fixed light-front time τ .

A key step in the analysis of an atomic system such as positronium is the introduction of the spherical coordinates r, θ, ϕ which separates the dynamics of Coulomb binding from the kinematical effects of the quantized orbital angular momentum L . The essential dynamics of the atom is specified by the radial Schrödinger equation whose eigensolutions $\psi_{n,L}(r)$ determine the bound-state wavefunction and eigenspectrum. In our recent work, [2] we have shown that there is an analogous invariant light-front coordinate ζ which allows one to separate the essential dynamics of quark and gluon binding from the kinematical physics of constituent spin and internal orbital angular momentum. The result is the single-variable LF Schrödinger equation for QCD Eq. 1, which determines the eigenspectrum and the light-front wavefunctions (LFWFs) of hadrons for general spin and orbital angular momentum. [2] If one further chooses the constituent rest frame (CRF) [3, 4, 5] where the total 3-momentum vanishes: $\sum_{i=1}^n \mathbf{k}_i = 0$, then the kinetic energy in the LF wave equation displays the usual 3-dimensional rotational invariance. Note that if the binding energy is nonzero, $P^z \neq 0$, in this frame.

The meson spectrum predicted by Eq. 1 has a string-theory Regge form $\mathcal{M}^2 =$

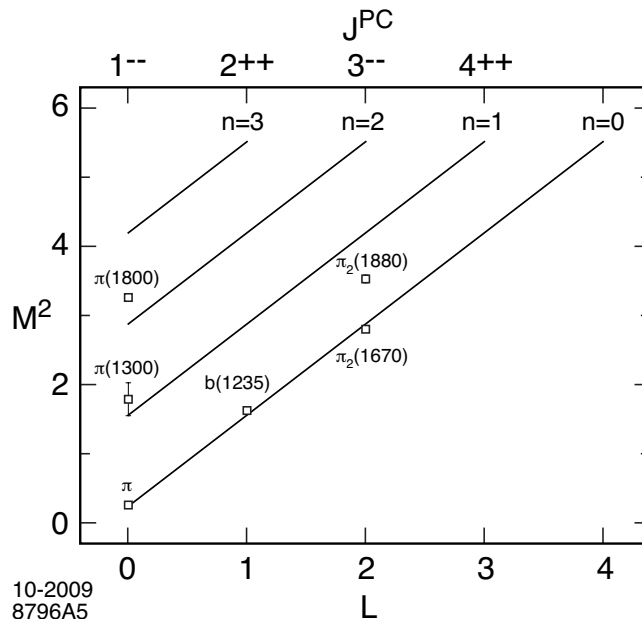


Figure 1: Parent and daughter Regge trajectories for the π -meson family for $\kappa = 0.6$ GeV.

$4\kappa^2(n+L+S/2)$; *i.e.*, the square of the eigenmasses are linear in both L and n , where n counts the number of nodes of the wavefunction in the radial variable ζ . This is illustrated for the pseudoscalar and vector meson spectra in Figs. 1 and 2, where the data are from Ref. [6]. The pion ($S = 0, n = 0, L = 0$) is massless for zero quark mass, consistent with chiral invariance. Thus one can compute the hadron spectrum by simply adding $4\kappa^2$ for a unit change in the radial quantum number, $4\kappa^2$ for a change in one unit in the orbital quantum number and $2\kappa^2$ for a change of one unit of spin S . Remarkably, the same rule holds for three-quark baryons as we shall show below. For other recent calculations of the hadronic spectrum based on AdS/QCD, see Refs. [7, 8, 9, 10, 11, 12, 13, 14, 15, 16, 17, 18, 19, 20].

The eigensolutions of Eq. 1 provide the light-front wavefunctions of the valence Fock state of the hadrons $\psi(\zeta) = \psi(x, \mathbf{b}_\perp)$ as illustrated for the pion in Fig. 3 for the soft and hard wall models. Given these wavefunctions one can predict many hadronic observables such as the generalized parton distributions that enter deeply virtual Compton scattering. For example, hadron form factors can be predicted from the overlap of LFWFs as in the Drell-Yan West formula. The prediction for the space-like pion form factor is shown in Fig. 4. The pion form factor and the vector meson poles residing in the dressed current in the soft wall model require choosing a value of κ smaller by a factor of $1/\sqrt{2}$ than the canonical value of κ which determines

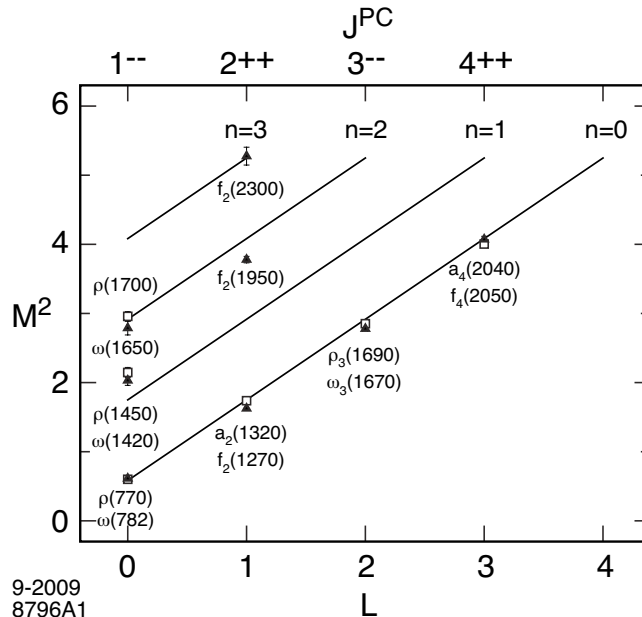


Figure 2: Regge trajectories for the $I=1$ ρ -meson and the $I=0$ ω -meson families for $\kappa = 0.54$ GeV.

the mass scale of the hadronic spectra. This shift is apparently due to the fact that the transverse current in $e^+e^- \rightarrow q\bar{q}$ creates a quark pair with $L^z = \pm 1$ instead of the $L^z = 0$ $q\bar{q}$ composition of the vector mesons in the spectrum. We will discuss this further in an upcoming paper. Other recent computations of the space-like pion form factor in AdS/QCD are presented in [24, 25]. Given the LFWFs one can compute jet hadronization at the amplitude level from first principles. [26] A similar method has been used to predict the production of antihydrogen from the off-shell coalescence of relativistic antiprotons and positrons. [27]

This semi-classical first approximation to QCD can be systematically improved by using the complete orthonormal solutions of Eq. 1 to diagonalize the QCD light-front Hamiltonian [28] or by applying the Lippmann-Schwinger method to systematically include the QCD interaction terms. In either case, the result is the full Fock state structure of the hadron eigensolution. One can also model heavy-light and heavy hadrons by including non-zero quark masses in the LF kinetic energy $\sum_i(\mathbf{k}_{\perp i}^2 + m_i^2)/x_i$ as well as the effects of the one-gluon exchange potential.

One can derive these results in two parallel ways. In the first method, one begins with a conformal approximation to QCD, justified by evidence that the theory has an infrared fixed point. [29] One then uses the fact that the conformal group has a geometrical representation in the five-dimensional AdS_5 space to model an effec-

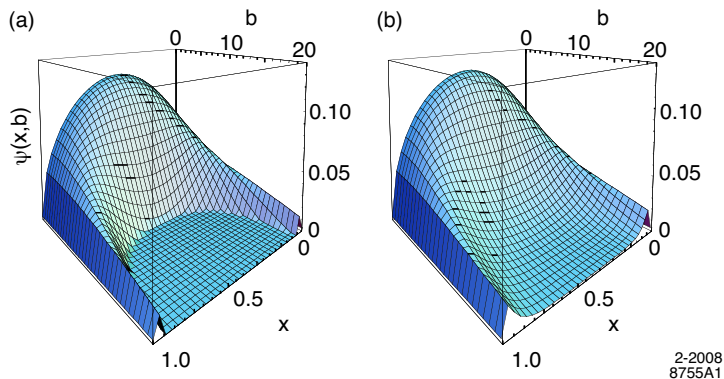


Figure 3: Pion light-front wavefunction $\psi_\pi(x, \mathbf{b}_\perp)$ for the AdS/QCD (a) hard-wall ($\Lambda_{QCD} = 0.32$ GeV) and (b) soft-wall ($\kappa = 0.375$ GeV) models.

tive dual gravity description in AdS. The fact that conformal invariance is reflected in the isometries of AdS is an essential ingredient of Maldacena’s AdS/CFT correspondence. Confinement is effectively introduced with a sharp cut-off in the infrared region of AdS space, the “hard-wall” model, [30] or with a dilaton background in the fifth dimension which produces a smooth cutoff and linear Regge trajectories, the “soft-wall” model. [31] The soft-wall AdS/CFT model with a dilaton-modified AdS space leads to the potential $U(z) = \kappa^4 z^2 + 2\kappa^2(L + S - 1)$. This potential can be derived directly from the action in AdS space [32] and corresponds to a dilaton profile $\exp(+\kappa^2 z^2)$, with opposite sign to that of Ref. [31]. The introduction of a positive dilaton profile is also relevant for describing chiral symmetry breaking, [33] since the expectation value of the scalar field associated with the quark mass and condensate does not blow up in the far infrared region of AdS in contrast with the original model. [31] Glazek and Schaden [34] have shown that a harmonic oscillator confining potential naturally arises as an effective potential between heavy quark states when one stochastically eliminates higher gluonic Fock states. Also, Hoyer [35] has argued that the Coulomb and a linear potentials are uniquely allowed in the Dirac equation at the classical level. The linear potential becomes a harmonic oscillator potential in the corresponding Klein-Gordon equation.

Hadrons are identified by matching the power behavior of the hadronic amplitude at the AdS boundary at small z to the twist of its interpolating operator at short distances $x^2 \rightarrow 0$, as required by the AdS/CFT dictionary. The twist corresponds to the dimension of fields appearing in chiral super-multiplets. [36] The twist of a hadron equals the number of constituents. We then apply light-front holography to relate the amplitude eigensolutions in the fifth dimension coordinate z to the LF wavefunctions in the physical spacetime variable ζ . Light-front holography can be derived by establishing an identity between the Polchinski-Strassler formula for

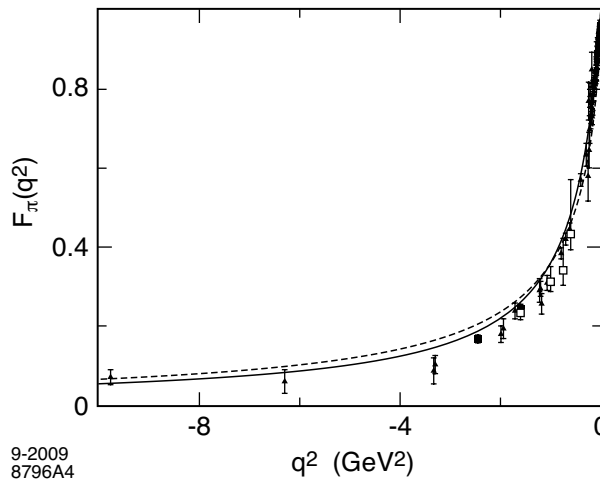


Figure 4: Space-like scaling behavior for $F_\pi(Q^2)$ as a function of q^2 . The continuous line is the prediction of the soft-wall model for $\kappa = 0.375$ GeV. The dashed line is the prediction of the hard-wall model for $\Lambda_{\text{QCD}} = 0.22$ GeV. The triangles are the data compilation from Baldini *et al.*, [21] the filled boxes are JLAB 1 data [22] and empty boxes are JLAB 2 data. [23]

current matrix elements and the corresponding Drell-Yan-West formula in LF theory. The same correspondence is obtained for both electromagnetic and gravitational form factors, a nontrivial test of consistency.

In the second method we use a first semiclassical approximation to transform the fixed LF time bound-state Hamiltonian equation to a corresponding wave equation in AdS space. The invariant LF coordinate ζ allows the separation of the dynamics of quark and gluon binding from the kinematics of constituent spin and internal orbital angular momentum. [2] In effect ζ represents the off-light-front energy shell or invariant mass dependence of the bound state. The result is the single-variable LF relativistic Schrödinger equation which determines the spectrum and LFWFs of hadrons for general spin and orbital angular momentum. This LF wave equation serves as a semiclassical first approximation to QCD, and it is equivalent to the equations of motion which describe the propagation of spin- J modes in AdS space.

The term $-(1-4L^2)/4\zeta^2$ in the LF equation of motion (1) is derived from the reduction of the LF kinetic energy when one transforms to the radial ζ and angular coordinate φ , in analogy to the $\ell(\ell+1)/r^2$ Casimir term in Schrödinger theory. One thus establishes the interpretation of L in the AdS equations of motion. The interaction terms build confinement and correspond to truncation of AdS space [2] in an effective dual gravity approximation. The duality between these two methods provides a direct connection between the description of hadronic modes in AdS space and the Hamiltonian formulation of QCD in physical space-time quantized on the

light-front at fixed LF time τ .

The identification of orbital angular momentum of the constituents is a key element in the description of the internal structure of hadrons using holographic principles. In our approach quark and gluon degrees of freedom are explicitly introduced in the gauge/gravity correspondence, in contrast with the usual AdS/QCD framework [37, 38] where axial and vector currents become the primary entities as in effective chiral theory. In our approach the holographic mapping is carried out in the strongly coupled regime where QCD is almost conformal corresponding to an infrared fixed-point. [29] Our analysis follows from recent developments in light-front QCD [39, 40, 41, 42, 43] which have been inspired by the AdS/CFT correspondence [44].

In the standard applications of AdS/CFT methods, one begins with Maldacena’s duality between the conformal supersymmetric $SO(4, 2)$ gauge theory and a semi-classical supergravity string theory defined in a 10 dimension $AdS_5 \times S^5$ space-time. There are no existing string theories actually dual to QCD, but nevertheless many interesting predictions can be made. In contrast, in our approach, we simply use the mathematical fact that the effects of scale transformations in a conformal theory can be mapped to the z dependence of amplitudes in AdS_5 space. QCD has an infrared fixed point and a conformal window in the infrared domain since the propagators of the confined quarks and gluons in the loop integrals contributing to the β function have a maximal wavelength. [45] Just as in QED, the β function must vanish in the IR. One then uses AdS_5 to represent scale transformations within the conformal window. Unlike the top-down supergravity approach, one is not limited to hadrons of maximum spin $J \leq 2$ in our bottom-up approach, and one can study baryons with $N_C = 3$.

2 The Light-Front Hamiltonian Approach to QCD

The Schrödinger wavefunction describes the quantum-mechanical structure of an atomic system at the amplitude level. Light-front wavefunctions play a similar role in quantum chromodynamics, providing a fundamental description of the structure and internal dynamics of hadrons in terms of their constituent quarks and gluons. The LFWFs of bound states in QCD are relativistic generalizations of the Schrödinger wavefunctions of atomic physics, but they are determined at fixed light-cone time $\tau = t + z/c$ – the “front form” introduced by Dirac [1] – rather than at fixed ordinary time t .

When a flash from a camera illuminates a scene, each object is illuminated along the light-front of the flash; i.e., at a given τ . Similarly, when a sample is illuminated by an x-ray source, each element of the target is struck at a given τ . In contrast, setting the initial condition using conventional instant time t requires simultaneous scattering

of photons on each constituent. Thus it is natural to set boundary conditions at fixed τ and then evolve the system using the light-front (LF) Hamiltonian $P^- = P^0 - P^3 = id/d\tau$. The invariant Hamiltonian $H_{LF} = P^+P^- - P_\perp^2$ then has eigenvalues \mathcal{M}^2 where \mathcal{M} is the physical mass. Its eigenfunctions are the light-front eigenstates whose Fock state projections define the light-front wavefunctions. Given the LF Fock state wavefunctions $\psi_n^H(x_i, \mathbf{k}_{\perp i}, \lambda_i)$, where $x_i = k^+/P^+$, $\sum_{i=1}^n x_i = 1$, $\sum_{i=1}^n \mathbf{k}_{\perp i} = 0$, one can immediately compute observables such as hadronic form factors (overlaps of LFWFs), structure functions (squares of LFWFs), as well as the generalized parton distributions and distribution amplitudes which underly hard exclusive reactions.

The most useful feature of LFWFs is the fact that they are frame independent; i.e., the form of the LFWF is independent of the hadron's total momentum $P^+ = P^0 + P^3$ and \mathbf{P}_\perp . The simplicity of Lorentz boosts of LFWFs contrasts dramatically with the complexity of the boost of wavefunctions defined at fixed time t . [46] Light-front quantization is thus the ideal framework to describe the structure of hadrons in terms of their quark and gluon degrees of freedom. The constituent spin and orbital angular momentum properties of the hadrons are also encoded in the LFWFs. The total angular momentum projection [47], $J^z = \sum_{i=1}^n S_i^z + \sum_{i=1}^{n-1} L_i^z$, is conserved Fock-state by Fock-state and by every interaction in the LF Hamiltonian. Other advantageous features of light-front quantization include:

- The simple structure of the light-front vacuum allows an unambiguous definition of the partonic content of a hadron in QCD. The chiral and gluonic condensates are properties of the higher Fock states, [48, 49] rather than the vacuum. In the case of the Higgs model, the effect of the usual Higgs vacuum expectation value is replaced by a constant $k^+ = 0$ zero mode field. [50]
- If one quantizes QCD in the physical light-cone gauge (LCG) $A^+ = 0$, then gluons only have physical angular momentum projections $S^z = \pm 1$. The orbital angular momenta of quarks and gluons are defined unambiguously, and there are no ghosts.
- The gauge-invariant distribution amplitude $\phi(x, Q)$ is the integral of the valence LFWF in LCG integrated over the internal transverse momentum $k_\perp^2 < Q^2$ because the Wilson line is trivial in this gauge. It is also possible to quantize QCD in Feynman gauge in the light front. [51]
- LF Hamiltonian perturbation theory provides a simple method for deriving analytic forms for the analog of Parke-Taylor amplitudes [52] where each particle spin S^z is quantized in the LF z direction. The gluonic g^6 amplitude $T(-1-1 \rightarrow +1+1+1+1+1+1)$ requires $\Delta L^z = 8$; it thus must vanish at tree level since each three-gluon vertex has $\Delta L^z = \pm 1$. However, the order g^8 one-loop amplitude can be nonzero.

- Amplitudes in light-front perturbation theory are automatically renormalized using the “alternate denominator” subtraction method. [53] The application to QED has been checked at one and two loops. [53]
- One can easily show using LF quantization that the anomalous gravitomagnetic moment $B(0)$ of a nucleon, as defined from the spin flip matrix element of the gravitational current, vanishes Fock-state by Fock state [47], as required by the equivalence principle. [54]
- LFWFs obey the cluster decomposition theorem, providing an elegant proof of this theorem for relativistic bound states. [55]
- The LF Hamiltonian can be diagonalized using the discretized light-cone quantization (DLCQ) method. [56] This nonperturbative method is particularly useful for solving low-dimension quantum field theories such as QCD(1 + 1). [57]
- LF quantization provides a distinction between static (the square of LFWFs) distributions versus non-universal dynamic structure functions, such as the Sivers single-spin correlation and diffractive deep inelastic scattering which involve final state interactions. The origin of nuclear shadowing and process independent anti-shadowing also becomes explicit.
- LF quantization provides a simple method to implement jet hadronization at the amplitude level.
- The instantaneous fermion interaction in LF quantization provides a simple derivation of the $J = 0$ fixed pole contribution to deeply virtual Compton scattering, [58] i.e., the $e_q^2 s^0 F(t)$ contribution to the DVCS amplitude which is independent of photon energy and virtuality.
- Unlike instant time quantization, the bound state Hamiltonian equation of motion in the LF is frame independent. This makes a direct connection of QCD with AdS/CFT methods possible. [2]

3 The Light-Front Hamiltonian

Light-front quantization of QCD provides a nonperturbative method for solving QCD in Minkowski space. Unlike lattice gauge theories, fermions introduce no new complications.

We can define the LF Lorentz invariant Hamiltonian $H_{LF} = P_\mu P^\mu = P^- P^+ - \mathbf{P}_\perp^2$ with eigenstates $|\psi_H(P^+, \mathbf{P}_\perp, S_z)\rangle$ and eigenmass \mathcal{M}_H^2 , the mass spectrum of the color-singlet states of QCD [59]

$$H_{LF}|\psi_H\rangle = \mathcal{M}_H^2|\psi_H\rangle. \quad (2)$$

A state $|\psi_H\rangle$ is an expansion in multi-particle Fock states $|n\rangle$ of the free LF Hamiltonian: $|\psi_H\rangle = \sum_n \psi_{n/H}|n\rangle$, where a one parton state is $|q\rangle = \sqrt{2q^+} b^\dagger(q)|0\rangle$. The Fock components $\psi_{n/H}(x_i, \mathbf{k}_{\perp i}, \lambda_i^z)$ are independent of P^+ and \mathbf{P}_\perp and depend only on relative partonic coordinates: the momentum fraction $x_i = k_i^+/P^+$, the transverse momentum $\mathbf{k}_{\perp i}$ and spin component λ_i^z . The LFWFs $\psi_{n/H}$ provide a *frame-independent* representation of a hadron which relates its quark and gluon degrees of freedom to their asymptotic hadronic state.

One can derive light-front holography using a first semiclassical approximation to transform the fixed light-front time bound-state Hamiltonian equation of motion in QCD to a corresponding wave equation in AdS space. [2] To this end we compute the invariant hadronic mass \mathcal{M}^2 from the hadronic matrix element

$$\langle\psi_H(P')|H_{LF}|\psi_H(P)\rangle = \mathcal{M}_H^2 \langle\psi_H(P')|\psi_H(P)\rangle, \quad (3)$$

expanding the initial and final hadronic states in terms of its Fock components. We use the frame $P = (P^+, M^2/P^+, \vec{0}_\perp)$ where $H_{LF} = P^+P^-$. The LF expression for \mathcal{M}^2 in impact space is

$$\mathcal{M}_H^2 = \sum_n \prod_{j=1}^{n-1} \int dx_j d^2\mathbf{b}_{\perp j} \psi_n^*(x_j, \mathbf{b}_{\perp j}) \sum_q \left(\frac{-\nabla_{\mathbf{b}_{\perp q}}^2 + m_q^2}{x_q} \right) \psi_n(x_j, \mathbf{b}_{\perp j}) + (\text{interactions}), \quad (4)$$

plus similar terms for antiquarks and gluons ($m_g = 0$).

To simplify the discussion we will consider a two-parton hadronic bound state. In the limit of zero quark mass $m_q \rightarrow 0$

$$\mathcal{M}^2 = \int_0^1 \frac{dx}{x(1-x)} \int d^2\mathbf{b}_\perp \psi^*(x, \mathbf{b}_\perp) (-\nabla_{\mathbf{b}_\perp}^2) \psi(x, \mathbf{b}_\perp) + (\text{interactions}). \quad (5)$$

The functional dependence for a given Fock state is given in terms of the invariant mass

$$\mathcal{M}_n^2 = \left(\sum_{a=1}^n k_a^\mu \right)^2 = \sum_a \frac{\mathbf{k}_{\perp a}^2 + m_a^2}{x_a} \rightarrow \frac{\mathbf{k}_\perp^2}{x(1-x)}, \quad (6)$$

the measure of the off-mass shell energy $\mathcal{M}^2 - \mathcal{M}_n^2$ of the bound state. Similarly in impact space the relevant variable for a two-parton state is $\zeta^2 = x(1-x)\mathbf{b}_\perp^2$. Thus, to first approximation LF dynamics depend only on the boost invariant variable \mathcal{M}_n or ζ , and hadronic properties are encoded in the hadronic mode $\phi(\zeta)$ from the relation

$$\psi(x, \zeta, \varphi) = e^{iM\varphi} X(x) \frac{\phi(\zeta)}{\sqrt{2\pi\zeta}}, \quad (7)$$

thus factoring out the angular dependence φ and the longitudinal, $X(x)$, and transverse mode $\phi(\zeta)$ with normalization $\langle\phi|\phi\rangle = \int d\zeta |\langle\zeta|\phi\rangle|^2 = 1$.

We can write the Laplacian operator in (5) in circular cylindrical coordinates (ζ, φ) and factor out the angular dependence of the modes in terms of the $SO(2)$ Casimir representation L^2 of orbital angular momentum in the transverse plane. Using (7) we find [2]

$$\mathcal{M}^2 = \int d\zeta \phi^*(\zeta) \sqrt{\zeta} \left(-\frac{d^2}{d\zeta^2} - \frac{1}{\zeta} \frac{d}{d\zeta} + \frac{L^2}{\zeta^2} \right) \frac{\phi(\zeta)}{\sqrt{\zeta}} + \int d\zeta \phi^*(\zeta) U(\zeta) \phi(\zeta), \quad (8)$$

where all the complexity of the interaction terms in the QCD Lagrangian is summed up in the effective potential $U(\zeta)$. The LF eigenvalue equation $H_{LF}|\phi\rangle = \mathcal{M}^2|\phi\rangle$ is thus a light-front wave equation for ϕ

$$\left(-\frac{d^2}{d\zeta^2} - \frac{1 - 4L^2}{4\zeta^2} + U(\zeta) \right) \phi(\zeta) = \mathcal{M}^2 \phi(\zeta), \quad (9)$$

an effective single-variable light-front Schrödinger equation which is relativistic, covariant and analytically tractable. It is important to notice that in the light-front the $SO(2)$ Casimir for orbital angular momentum L^2 is a kinematical quantity, in contrast with the usual $SO(3)$ Casimir $\ell(\ell+1)$ from non-relativistic physics which is rotational, but not boost invariant. Using (4) one can readily generalize the equations to allow for the kinetic energy of massive quarks. [60] In this case, however, the longitudinal mode $X(x)$ does not decouple from the effective LF bound-state equations.

As the simplest example, we consider a bag-like model where partons are free inside the hadron and the interaction terms effectively build confinement. The effective potential is a hard wall: $U(\zeta) = 0$ if $\zeta \leq 1/\Lambda_{\text{QCD}}$ and $U(\zeta) = \infty$ if $\zeta > 1/\Lambda_{\text{QCD}}$, where boundary conditions are imposed on the boost invariant variable ζ at fixed light-front time. If $L^2 \geq 0$ the LF Hamiltonian is positive definite $\langle \phi | H_{LF} | \phi \rangle \geq 0$ and thus $\mathcal{M}^2 \geq 0$. If $L^2 < 0$ the bound state equation is unbounded from below and the particle “falls towards the center”. The critical value corresponds to $L = 0$. The mode spectrum follows from the boundary conditions $\phi(\zeta = 1/\Lambda_{\text{QCD}}) = 0$, and is given in terms of the roots of Bessel functions: $\mathcal{M}_{L,k} = \beta_{L,k} \Lambda_{\text{QCD}}$. Upon the substitution $\Phi(\zeta) \sim \zeta^{3/2} \phi(\zeta)$, $\zeta \rightarrow z$ we find

$$[z^2 \partial_z^2 - 3z \partial_z + z^2 \mathcal{M}^2 - (\mu R)^2] \Phi_J = 0, \quad (10)$$

the wave equation which describes the propagation of a scalar mode in a fixed AdS_5 background with AdS radius R . The five dimensional mass μ is related to the orbital angular momentum of the hadronic bound state by $(\mu R)^2 = -4 + L^2$. The quantum mechanical stability $L^2 > 0$ is thus equivalent to the Breitenlohner-Freedman stability bound in AdS. [61] The scaling dimensions are $\Delta = 2 + L$ independent of J in agreement with the twist scaling dimension of a two parton bound state in QCD. Higher spin- J wave equations are obtained by shifting dimensions: $\Phi_J(z) = (z/R)^{-J} \Phi(z)$. [2]

The hard-wall LF model discussed here is equivalent to the hard wall model of Ref. [30]. The variable ζ , $0 \leq \zeta \leq \Lambda_{\text{QCD}}^{-1}$, represents the invariable separation between pointlike constituents and is also the holographic variable z in AdS, thus we can identify $\zeta = z$. Likewise a two-dimensional oscillator with effective potential $U(z) = \kappa^4 z^2 + 2\kappa^2(L + S - 1)$ is similar to the soft-wall model of Ref. [31] which reproduce the usual linear Regge trajectories, where L is the internal orbital angular momentum and S is the internal spin. The soft-wall discussed here correspond to a positive sign dilaton [32, 33], and higher-spin solutions follow from shifting dimensions: $\Phi_J(z) = (z/R)^{-J}\Phi(z)$.

Individual hadron states can be identified by their interpolating operator at $z \rightarrow 0$. For example, the pseudoscalar meson interpolating operator $\mathcal{O}_{2+L} = \bar{q}\gamma_5 D_{\{\ell_1} \cdots D_{\ell_m\}} q$, written in terms of the symmetrized product of covariant derivatives D with total internal orbital momentum $L = \sum_{i=1}^m \ell_i$, is a twist-two, dimension $3 + L$ operator with scaling behavior determined by its twist-dimension $2 + L$. Likewise the vector-meson operator $\mathcal{O}_{2+L}^\mu = \bar{q}\gamma^\mu D_{\{\ell_1} \cdots D_{\ell_m\}} q$ has scaling dimension $\Delta = 2 + L$. The scaling behavior of the scalar and vector AdS modes $\Phi(z) \sim z^\Delta$ at $z \rightarrow 0$ is precisely the scaling required to match the scaling dimension of the local pseudoscalar and vector-meson interpolating operators. The spectral predictions for the light pseudoscalar and vector mesons in the Chew-Frautschi plot in Fig. 1 and 2 for the soft-wall model discussed here are in good agreement for the principal and daughter Regge trajectories. Radial excitations correspond to the nodes of the wavefunction.

For baryons, the light-front wave equation is a linear equation determined by the LF transformation properties of spin 1/2 states. A linear confining potential $U(\zeta) \sim \kappa^2 \zeta$ in the LF Dirac equation leads to linear Regge trajectories. [60] For fermionic modes the light-front matrix Hamiltonian eigenvalue equation $D_{LF}|\psi\rangle = \mathcal{M}|\psi\rangle$, $H_{LF} = D_{LF}^2$, in a 2×2 spinor component representation is equivalent to the system of coupled linear equations

$$\begin{aligned} -\frac{d}{d\zeta}\psi_- - \frac{\nu + \frac{1}{2}}{\zeta}\psi_- - \kappa^2\zeta\psi_- &= \mathcal{M}\psi_+, \\ \frac{d}{d\zeta}\psi_+ - \frac{\nu + \frac{1}{2}}{\zeta}\psi_+ - \kappa^2\zeta\psi_+ &= \mathcal{M}\psi_-. \end{aligned} \quad (11)$$

with eigenfunctions

$$\begin{aligned} \psi_+(\zeta) &\sim z^{\frac{1}{2}+\nu} e^{-\kappa^2\zeta^2/2} L_n^\nu(\kappa^2\zeta^2), \\ \psi_-(\zeta) &\sim z^{\frac{3}{2}+\nu} e^{-\kappa^2\zeta^2/2} L_n^{\nu+1}(\kappa^2\zeta^2), \end{aligned} \quad (12)$$

and eigenvalues

$$\mathcal{M}^2 = 4\kappa^2(n + \nu + 1). \quad (13)$$

The baryon interpolating operator $\mathcal{O}_{3+L} = \psi D_{\{\ell_1} \cdots D_{\ell_q} \psi D_{\ell_{q+1}} \cdots D_{\ell_m\}} \psi$, $L = \sum_{i=1}^m \ell_i$ is a twist 3, dimension $9/2 + L$ with scaling behavior given by its twist-dimension $3 + L$. We thus require $\nu = L + 1$ to match the short distance scaling

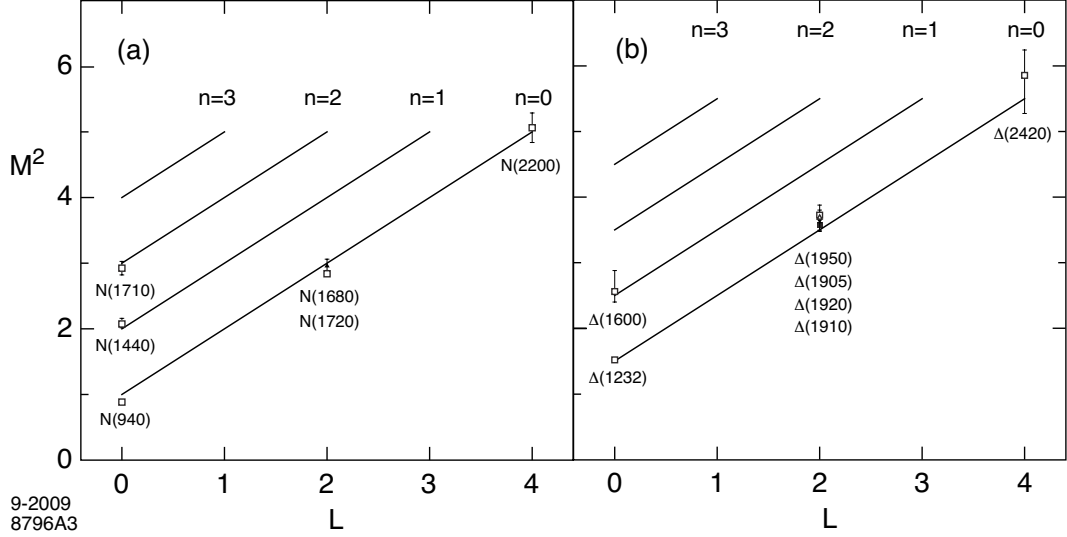


Figure 5: **56** Regge trajectories for the N and Δ baryon families for $\kappa = 0.5$ GeV

behavior. Higher spin fermionic modes are obtained by shifting dimensions for the fields as in the bosonic case. Thus, as in the meson sector, the increase in the mass squared for higher baryonic state is $\Delta n = 4\kappa^2$, $\Delta L = 4\kappa^2$ and $\Delta S = 2\kappa^2$, relative to the lowest ground state, the proton.

The predictions for the **56**-plet of light baryons under the $SU(6)$ flavor group are shown in Fig. 5. As for the predictions for mesons in Fig. 2, only confirmed PDG [6] states are shown. The Roper state $N(1440)$ and the $N(1710)$ are well accounted for in this model as the first and second radial states. Likewise the $\Delta(1660)$ corresponds to the first radial state of the Δ family. The model is successful in explaining the important parity degeneracy observed in the light baryon spectrum, such as the $L = 2$, $N(1680) - N(1720)$ degenerate pair and the $L = 2$, $\Delta(1905), \Delta(1910), \Delta(1920), \Delta(1950)$ states which are degenerate within error bars. Parity degeneracy of baryons is also a property of the hard wall model, but radial states are not well described in this model. [40]

4 Holographic Mapping of Transition Amplitudes

Light-Front Holography can also be derived by observing the correspondence between matrix elements obtained in AdS/CFT with the corresponding formula using the LF representation. [41] The light-front electromagnetic form factor in impact space [41, 42, 62] can be written as a sum of overlap of light-front wave functions of the $j =$

1, 2, \dots , $n - 1$ spectator constituents:

$$F(q^2) = \sum_n \prod_{j=1}^{n-1} \int dx_j d^2 \mathbf{b}_{\perp j} \sum_q e_q \exp\left(i \mathbf{q}_{\perp} \cdot \sum_{j=1}^{n-1} x_j \mathbf{b}_{\perp j}\right) |\psi_n(x_j, \mathbf{b}_{\perp j})|^2 \quad (14)$$

where the normalization is defined by

$$\sum_n \prod_{j=1}^{n-1} \int dx_j d^2 \mathbf{b}_{\perp j} |\psi_{n/H}(x_j, \mathbf{b}_{\perp j})|^2 = 1. \quad (15)$$

The formula is exact if the sum is over all Fock states n . For definiteness we shall consider a two-quark π^+ valence Fock state $|u\bar{d}\rangle$ with charges $e_u = \frac{2}{3}$ and $e_{\bar{d}} = \frac{1}{3}$. For $n = 2$, there are two terms which contribute to the q -sum in (14). Exchanging $x \leftrightarrow 1 - x$ in the second integral we find

$$F_{\pi^+}(q^2) = 2\pi \int_0^1 \frac{dx}{x(1-x)} \int \zeta d\zeta J_0\left(\zeta q \sqrt{\frac{1-x}{x}}\right) \left| \psi_{u\bar{d}/\pi}(x, \zeta) \right|^2, \quad (16)$$

where $\zeta^2 = x(1-x)\mathbf{b}_{\perp}^2$ and $F_{\pi^+}(q=0) = 1$.

We now compare this result with the electromagnetic form-factor in AdS space: [63]

$$F(Q^2) = R^3 \int \frac{dz}{z^3} J(Q^2, z) |\Phi(z)|^2, \quad (17)$$

where $J(Q^2, z) = zQK_1(zQ)$. Using the integral representation of $J(Q^2, z)$

$$J(Q^2, z) = \int_0^1 dx J_0\left(\zeta Q \sqrt{\frac{1-x}{x}}\right), \quad (18)$$

we write the AdS electromagnetic form-factor as

$$F(Q^2) = R^3 \int_0^1 dx \int \frac{dz}{z^3} J_0\left(zQ \sqrt{\frac{1-x}{x}}\right) |\Phi(z)|^2. \quad (19)$$

Comparing with the light-front QCD form factor (16) for arbitrary values of Q [41]

$$|\psi(x, \zeta)|^2 = \frac{R^3}{2\pi} x(1-x) \frac{|\Phi(\zeta)|^2}{\zeta^4}, \quad (20)$$

where we identify the transverse LF variable ζ , $0 \leq \zeta \leq \Lambda_{\text{QCD}}$, with the holographic variable z . Identical results are obtained from the mapping of the QCD gravitational form factor with the expression for the hadronic gravitational form factor in AdS space. [43, 64]

5 Vacuum Effects and Light-Front Quantization

The LF vacuum is remarkably simple in light-cone quantization because of the restriction $k^+ \geq 0$. For example in QED, vacuum graphs such as $e^+e^-\gamma$ associated with the zero-point energy do not arise. In the Higgs theory, the usual Higgs vacuum expectation value is replaced with a $k^+ = 0$ zero mode [50]; however, the resulting phenomenology is identical to the standard analysis.

Hadronic condensates play an important role in quantum chromodynamics (QCD). Conventionally, these condensates are considered to be properties of the QCD vacuum and hence to be constant throughout spacetime. A new perspective on the nature of QCD condensates $\langle \bar{q}q \rangle$ and $\langle G_{\mu\nu}G^{\mu\nu} \rangle$, particularly where they have spatial and temporal support, has recently been presented. [45, 49, 65, 66] Their spatial support is restricted to the interior of hadrons, since these condensates arise due to the interactions of quarks and gluons which are confined within hadrons. For example, consider a meson consisting of a light quark q bound to a heavy antiquark, such as a B meson. One can analyze the propagation of the light q in the background field of the heavy \bar{b} quark. Solving the Dyson-Schwinger equation for the light quark one obtains a nonzero dynamical mass and, via the connection mentioned above, hence a nonzero value of the condensate $\langle \bar{q}q \rangle$. But this is not a true vacuum expectation value; instead, it is the matrix element of the operator $\bar{q}q$ in the background field of the \bar{b} quark. The change in the (dynamical) mass of the light quark in this bound state is somewhat reminiscent of the energy shift of an electron in the Lamb shift, in that both are consequences of the fermion being in a bound state rather than propagating freely. Similarly, it is important to use the equations of motion for confined quarks and gluon fields when analyzing current correlators in QCD, not free propagators, as has often been done in traditional analyses of operator products. Since the distance between the quark and antiquark cannot become arbitrarily large, one cannot create a quark condensate which has uniform extent throughout the universe. The 45 orders of magnitude conflict of QCD with the observed value of the cosmological condensate is thus removed. [66] A new perspective on the nature of quark and gluon condensates in quantum chromodynamics is thus obtained: [45, 65, 66] the spatial support of QCD condensates is restricted to the interior of hadrons, since they arise due to the interactions of confined quarks and gluons. In LF theory, the condensate physics is replaced by the dynamics of higher non-valence Fock states as shown by Casher and Susskind. [48] In particular, chiral symmetry is broken in a limited domain of size $1/m_\pi$, in analogy to the limited physical extent of superconductor phases. This novel description of chiral symmetry breaking in terms of “in-hadron condensates” has also been observed in Bethe-Salpeter studies. [67, 68] This picture also explains the results of recent studies [69, 70, 71] which find no significant signal for the vacuum gluon condensate.

AdS/QCD also provides a description of chiral symmetry breaking by using the

propagation of a scalar field $X(z)$ to represent the dynamical running quark mass. The AdS solution has the form [37, 38] $X(z) = a_1 z + a_2 z^3$, where a_1 is proportional to the current-quark mass. The coefficient a_2 scales as Λ_{QCD}^3 and is the analog of $\langle \bar{q}q \rangle$; however, since the quark is a color nonsinglet, the propagation of $X(z)$, and thus the domain of the quark condensate, is limited to the region of color confinement. Furthermore the effect of the a_2 term varies within the hadron, as characteristic of an in-hadron condensate. A similar solution is found in the soft wall model in presence of a positive sign dilaton. [33] The AdS/QCD picture of condensates with spatial support restricted to hadrons is also in general agreement with results from chiral bag models [72, 73, 74], which modify the original MIT bag by coupling a pion field to the surface of the bag in a chirally invariant manner.

6 Conclusions

We have derived a connection between a semiclassical first approximation to QCD, quantized on the light-front, and hadronic modes propagating on a fixed AdS background. This leads to an effective relativistic Schrödinger-like equation in the AdS fifth dimension coordinate z (1). We have show how this identical AdS wave equation can be derived in physical space time as an effective equation for valence quarks in LF quantized theory, where one identifies the AdS fifth dimension coordinate z with the LF coordinate ζ . We originally derived this correspondence using the identity between electromagnetic and gravitational form factors computed in AdS and LF theory [41, 42, 43]. Our derivation shows that the fifth-dimensional mass μ in the AdS equation of motion is directly related to orbital angular momentum L in physical space-time. The result is physically compelling and phenomenologically successful.

We have shown how the soft-wall AdS/CFT model with a dilaton-modified AdS space leads to the potential $U(z) = \kappa^4 z^2 + 2\kappa^2(L+S-1)$. This potential can be derived directly from the action in AdS space and corresponds to a dilaton profile $\exp(+\kappa^2 z^2)$, with opposite sign to that of Ref. [31]. Hadrons are identified by matching the power behavior of the hadronic amplitude at the AdS boundary at small z to the twist of its interpolating operator at short distances $x^2 \rightarrow 0$, as required by the AdS/CFT dictionary. The twist corresponds to the dimension of fields appearing in chiral supermultiplets. The twist of a hadron equals the number of constituents.

The Schrödinger-like light-front AdS/QCD equation provides successful predictions for the light-quark meson and baryon spectra, as function of hadron spin, quark angular momentum, and radial quantum number. [75] The pion is massless for zero mass quarks in agreement with chiral invariance arguments. The predictions for form factors are also successful. The predicted power law fall-off agrees with dimensional counting rules as required by conformal invariance at small z . [42, 60]

Higher spin modes follow from shifting dimensions in the AdS wave equations.

In the hard-wall model the dependence is linear: $\mathcal{M} \sim 2n + L$. In the soft-wall model the usual Regge behavior is found $\mathcal{M}^2 \sim n + L$. Both models predict the same multiplicity of states for mesons and baryons as observed experimentally. [76] It is possible to extend the model to hadrons with heavy quark constituents by introducing nonzero quark masses and short-range Coulomb corrections.

The AdS/QCD semiclassical approximation to light-front QCD does not account for particle creation and absorption, and thus it will break down at short distances where hard gluon exchange and quantum corrections become important. However, the model can be systematically improved by using its complete orthonormal solutions to diagonalize the QCD light-front Hamiltonian [28] or by applying the Lippmann-Schwinger method to systematically include the QCD interaction terms.

Acknowledgments

Presented by SJB at the 10th Workshop on Non-Perturbative QCD at the Institut d'Astrophysique de Paris (IAP), June 8-12, 2009. We thank Carl Carlson, Alexandre Deur, Josh Erlich, Stan Glazek, Paul Hoyer, Eberhard Klempt, Craig Roberts, Robert Shrock, James Vary, and Fen Zuo for helpful conversations and collaborations. Section 3 is based on collaborations with Robert Shrock. This research was supported by the Department of Energy contract DE-AC02-76SF00515. SLAC-PUB-13790.

References

- [1] P. A. M. Dirac, *Rev. Mod. Phys.* **21**, 392 (1949).
- [2] G. F. de Teramond and S. J. Brodsky, *Phys. Rev. Lett.* **102**, 081601 (2009) [arXiv:0809.4899 [hep-ph]].
- [3] P. Danielewicz and J. M. Namyslowski, *Phys. Lett. B* **81**, 110 (1979).
- [4] V. A. Karmanov, *Nucl. Phys. B* **166**, 378 (1980).
- [5] S. D. Glazek, *Acta Phys. Polon. B* **15**, 889 (1984).
- [6] C. Amsler *et al.* (Particle Data Group), *Phys. Lett. B* **667** (2008) 1.
- [7] H. Boschi-Filho and N. R. F. Braga, *JHEP* **0305**, 009 (2003) [arXiv:hep-th/0212207].
- [8] H. Boschi-Filho, N. R. F. Braga and H. L. Carrion, *Phys. Rev. D* **73**, 047901 (2006) [arXiv:hep-th/0507063].
- [9] N. Evans and A. Tedder, *Phys. Lett. B* **642**, 546 (2006) [arXiv:hep-ph/0609112].

- [10] D. K. Hong, T. Inami and H. U. Yee, Phys. Lett. B **646**, 165 (2007) [arXiv:hep-ph/0609270].
- [11] P. Colangelo, F. De Fazio, F. Jugeau and S. Nicotri, Phys. Lett. B **652**, 73 (2007) [arXiv:hep-ph/0703316].
- [12] H. Forkel, Phys. Rev. D **78**, 025001 (2008) [arXiv:0711.1179 [hep-ph]].
- [13] A. Vega and I. Schmidt, Phys. Rev. D **78** (2008) 017703 [arXiv:0806.2267 [hep-ph]].
- [14] K. Nawa, H. Suganuma and T. Kojo, Mod. Phys. Lett. A **23**, 2364 (2008) [arXiv:0806.3040 [hep-th]].
- [15] W. de Paula, T. Frederico, H. Forkel and M. Beyer, Phys. Rev. D **79**, 075019 (2009) [arXiv:0806.3830 [hep-ph]].
- [16] P. Colangelo, F. De Fazio, F. Giannuzzi, F. Jugeau and S. Nicotri, Phys. Rev. D **78** (2008) 055009 [arXiv:0807.1054 [hep-ph]].
- [17] H. Forkel and E. Klempt, Phys. Lett. B **679**, 77 (2009) [arXiv:0810.2959 [hep-ph]].
- [18] H. C. Ahn, D. K. Hong, C. Park and S. Siwach, arXiv:0904.3731 [hep-ph].
- [19] W. de Paula and T. Frederico, arXiv:0908.4282 [hep-ph].
- [20] Y. Q. Sui, Y. L. Wu, Z. F. Xie and Y. B. Yang, arXiv:0909.3887 [hep-ph].
- [21] R. Baldini, S. Dubnicka, P. Gauzzi, S. Pacetti, E. Pasqualucci and Y. Srivastava, Eur. Phys. J. C **11**, 709 (1999).
- [22] V. Tadevosyan *et al.* [Jefferson Lab F(pi) Collaboration], Phys. Rev. C **75**, 055205 (2007) [arXiv:nucl-ex/0607007].
- [23] T. Horn *et al.* [Fpi2 Collaboration], Phys. Rev. Lett. **97**, 192001 (2006) [arXiv:nucl-ex/0607005].
- [24] H. J. Kwee and R. F. Lebed, JHEP **0801**, 027 (2008) [arXiv:0708.4054 [hep-ph]]; Phys. Rev. D **77**, 115007 (2008) [arXiv:0712.1811 [hep-ph]].
- [25] H. R. Grigoryan and A. V. Radyushkin, Phys. Rev. D **76** (2007) 115007 [arXiv:0709.0500 [hep-ph]]; Phys. Rev. D **78** (2008) 115008 [arXiv:0808.1243 [hep-ph]].
- [26] S. J. Brodsky, G. de Teramond and R. Shrock, AIP Conf. Proc. **1056**, 3 (2008) [arXiv:0807.2484 [hep-ph]].

- [27] C. T. Munger, S. J. Brodsky and I. Schmidt, Phys. Rev. D **49**, 3228 (1994).
- [28] J. P. Vary *et al.*, arXiv:0905.1411 [nucl-th].
- [29] A. Deur, V. Burkert, J. P. Chen and W. Korsch, Phys. Lett. B **665**, 349 (2008) [arXiv:0803.4119 [hep-ph]].
- [30] J. Polchinski and M. J. Strassler, Phys. Rev. Lett. **88**, 031601 (2002) [arXiv:hep-th/0109174].
- [31] A. Karch, E. Katz, D. T. Son and M. A. Stephanov, Phys. Rev. D **74**, 015005 (2006) [arXiv:hep-ph/0602229].
- [32] G. F. de Teramond and S. J. Brodsky, arXiv:0909.3900 [hep-ph].
- [33] F. Zuo, arXiv:0909.4240 [hep-ph].
- [34] S. D. Glazek and M. Schaden, Phys. Lett. B **198**, 42 (1987).
- [35] P. Hoyer, arXiv:0909.3045 [hep-ph].
- [36] N. J. Craig and D. Green, arXiv:0905.4088 [hep-ph].
- [37] J. Erlich, E. Katz, D. T. Son and M. A. Stephanov, Phys. Rev. Lett. **95**, 261602 (2005) [arXiv:hep-ph/0501128].
- [38] L. Da Rold and A. Pomarol, Nucl. Phys. B **721**, 79 (2005) [arXiv:hep-ph/0501218].
- [39] S. J. Brodsky and G. F. de Teramond, Phys. Lett. B **582**, 211 (2004) [arXiv:hep-th/0310227].
- [40] G. F. de Teramond and S. J. Brodsky, Phys. Rev. Lett. **94**, 201601 (2005) [arXiv:hep-th/0501022].
- [41] S. J. Brodsky and G. F. de Teramond, Phys. Rev. Lett. **96**, 201601 (2006) [arXiv:hep-ph/0602252];
- [42] S. J. Brodsky and G. F. de Teramond, Phys. Rev. D **77**, 056007 (2008) [arXiv:0707.3859 [hep-ph]].
- [43] S. J. Brodsky and G. F. de Teramond, Phys. Rev. D **78**, 025032 (2008) [arXiv:0804.0452 [hep-ph]].
- [44] J. M. Maldacena, Adv. Theor. Math. Phys. **2**, 231 (1998) [Int. J. Theor. Phys. **38**, 1113 (1999)] [arXiv:hep-th/9711200].

- [45] S. J. Brodsky and R. Shrock, Phys. Lett. B **666**, 95 (2008) [arXiv:0806.1535 [hep-th]].
- [46] S. J. Brodsky and J. R. Primack, Annals Phys. **52**, 315 (1969).
- [47] S. J. Brodsky, D. S. Hwang, B. Q. Ma and I. Schmidt, Nucl. Phys. B **593**, 311 (2001) [arXiv:hep-th/0003082].
- [48] A. Casher and L. Susskind, Phys. Rev. D **9**, 436 (1974).
- [49] S. J. Brodsky and R. Shrock, arXiv:0905.1151 [hep-th].
- [50] P. P. Srivastava and S. J. Brodsky, Phys. Rev. D **66**, 045019 (2002) [arXiv:hep-ph/0202141].
- [51] P. P. Srivastava and S. J. Brodsky, Phys. Rev. D **61**, 025013 (2000) [arXiv:hep-ph/9906423].
- [52] L. Motyka and A. M. Stasto, arXiv:0901.4949 [hep-ph].
- [53] S. J. Brodsky, R. Roskies and R. Suaya, Phys. Rev. D **8**, 4574 (1973).
- [54] O. V. Teryaev, arXiv:hep-ph/9904376.
- [55] S. J. Brodsky and C. R. Ji, Phys. Rev. D **33**, 2653 (1986).
- [56] H. C. Pauli and S. J. Brodsky, Phys. Rev. D **32**, 2001 (1985).
- [57] K. Hornbostel, S. J. Brodsky and H. C. Pauli, Phys. Rev. D **41**, 3814 (1990).
- [58] S. J. Brodsky, F. J. Llanes-Estrada, J. T. Londergan and A. P. Szczepaniak, arXiv:0906.5515 [hep-ph].
- [59] S. J. Brodsky, H. C. Pauli and S. S. Pinsky, Phys. Rept. **301**, 299 (1998) [arXiv:hep-ph/9705477].
- [60] S. J. Brodsky and G. F. de Teramond, arXiv:0802.0514 [hep-ph].
- [61] P. Breitenlohner and D. Z. Freedman, Annals Phys. **144**, 249 (1982).
- [62] D. E. Soper, Phys. Rev. D **15**, 1141 (1977).
- [63] J. Polchinski and M. J. Strassler, JHEP **0305**, 012 (2003) [arXiv:hep-th/0209211].
- [64] Z. Abidin and C. E. Carlson, Phys. Rev. D **77**, 095007 (2008) [arXiv:0801.3839 [hep-ph]].

- [65] S. J. Brodsky and R. Shrock, arXiv:0803.2541 [hep-th].
- [66] S. J. Brodsky and R. Shrock, arXiv:0803.2554 [hep-th].
- [67] P. Maris, C. D. Roberts and P. C. Tandy, Phys. Lett. B **420**, 267 (1998) [arXiv:nucl-th/9707003].
- [68] P. Maris and C. D. Roberts, Phys. Rev. C **56**, 3369 (1997) [arXiv:nucl-th/9708029].
- [69] B. L. Ioffe and K. N. Zybalyuk, Eur. Phys. J. C **27**, 229 (2003) [arXiv:hep-ph/0207183].
- [70] M. Davier, A. Hocker and Z. Zhang, Nucl. Phys. Proc. Suppl. **169**, 22 (2007) [arXiv:hep-ph/0701170].
- [71] M. Davier, S. Descotes-Genon, A. Hocker, B. Malaescu and Z. Zhang, Eur. Phys. J. C **56**, 305 (2008) [arXiv:0803.0979 [hep-ph]].
- [72] A. Chodos and C. B. Thorn, Phys. Rev. D **12**, 2733 (1975).
- [73] G. E. Brown and M. Rho, Phys. Lett. B **82** (1979) 177.
- [74] A. Hosaka and H. Toki, Phys. Rept. **277**, 65 (1996).
- [75] The SU(6) **70**-plet of light baryons is not well described in this simple model, and further investigation is necessary. See: [17].
- [76] E. Klempt and A. Zaitsev, Phys. Rept. **454**, 1 (2007) [arXiv:0708.4016 [hep-ph]].